# Better Alternative to "Astronomical Silicate": Laboratory-Based Optical Functions of Chondritic/Solar Abundance Glass With Application to HD 161796

A. K. Speck
*Department of Physics and Astronomy, University of Missouri-Columbia, Columbia, MO 65211, USA*
speckan@missouri.edu

K. M. Pitman
*Planetary Science Institute, Tucson, AZ 85719, USA*
now at *Space Science Institute, Boulder, CO 80301, USA.*
and

A. M. Hofmeister
*Department of Earth and Planetary Sciences, Washington University, St. Louis, MO 63130, USA*

## ABSTRACT

"Astronomical" or "circumstellar" silicate optical functions (real and imaginary indices of refraction $n(\lambda)$ and $k(\lambda)$) have been previously derived from compositionally and structurally disparate samples; past values were compiled from different sources in the literature, and are essentially kluges of observational, laboratory, and extrapolated or interpolated values. These synthetic optical functions were created because astronomers lack the quantitative data on amorphous silicates at all wavelengths needed for radiative transfer modeling. This paper provides optical functions that (1) are created with a consistent methodology, (2) use the same sample across all wavelengths, and (3) minimize interpolation and extrapolation wherever possible. We present electronic data tables of optical functions derived from mid-ultraviolet to far-infrared laboratory transmission spectra for two materials: iron-free glass with chondritic/solar atmospheric abundances, and metallic iron. We compare these optical functions to other popular $n$, $k$ data used to model amorphous silicates (e.g., "astronomical" or "circumstellar" silicate), both directly and in application to a simple system: the dust shell of the post-AGB star HD 161796. Using the new optical functions, we find that the far-IR profile of model SEDs are significantly affected by the ratio of glass to iron. Our case study on HD161796 shows that modeling with our new optical functions, the mineralogy is markedly different from that derived using synthetic optical functions and suggests a new scenario of crystalline silicate formation.

*Subject headings:* (ISM;) dust, extinction – methods: laboratory – ultraviolet: ISM – infrared: ISM

## 1. Introduction

Silicate grains dominate the emission and extinction processes in many astrophysical environments but astronomers still do not know exactly what composition or structure constitutes these dust grains or how these properties change from location to location. Astromineralogy, the study of the precise and detailed nature of dust grains in space, has developed rapidly over the past few decades (see reviews in Speck et al. 1997; Speck 1998;

Speck et al. 2000; Molster 2000; Waters & Molster 1999; Henning 2003; Kwok 2004; Pitman et al. 2010; Guha Niyogi et al. 2011a; Speck 2012). However, interpretation of dust grains is still limited by the paucity and quality of mineral data used for comparison with and modeling of astronomical observations.

While dust in space is particulate in nature, there is some discussion about whether it is appropriate to use bulk materials for spectroscopy of candidate solids (e.g. Speck, Hofmeister & Barlow 1999; Henning 2003, and references therein). It has already been shown that thin films (slabs) and dilute particle distributions result in the same spectral features (Speck, Hofmeister & Barlow 1999). Moreover, having optical constants from spectra of bulk materials is important because they set an upper limit for extinction through a certain material (Hofmeister et al. 2009).

Although laboratory measurements of optical functions for astronomical applications are of high value, they characterize individual analogue materials and are not the real dust we see in space. However, good quality extinction properties of the components of the real space dust can be derived from these analogue materials. Likewise, deriving a set of effective optical functions from astronomical data would be acceptable if the temperature and density structure, and grain size and shape distribution of a system was well known. Here we aim to provide optical functions that allow us to determine these details in astronomical environments more completely.

There are two basic approaches to identifying dust minerals in space: (1) Work backward from astronomical observations where temperature and density structure of a system is well known to derive effective optical functions that approximate those of real dust in space. (2) Work forward from laboratory measurements of dust analogue minerals whose compositions and impurities are well characterized to derive optical functions of minerals predicted to occur in space.

Ideally, we should use both approaches and find where (1) and (2) match, however, astronomers do not take the dual approach. Approach (1) alone does not reveal anything about the chemistry; those optical functions are not useful for diagnosing changes from location to location and should not be used to interpret compositional effects elsewhere. We are taking approach (2) by providing dust analogue data that will provide insight into the chemistry. Moreover we are correcting past efforts which made kluges that hybridize rather than compare the two approaches.

The simplest approach for determining the nature of dust grains in space is to match the positions, widths, and strengths of observed spectral features with those seen in laboratory spectra. This is usually achieved by fitting a continuum to the observed spectrum and dividing (or subtracting) to derive emissivities of the observed spectral features. These emissivities are then compared to absorption spectra[1] produced in the laboratory. Sometimes the emission/absorption profile is calculated from optical functions (complex refractive indices; $n_\lambda$ and $k_\lambda$; see e.g. Guha Niyogi et al. 2011a)[2]. Radiative transfer (RT) modeling uses the optical functions[3] minerals to predict how a given object should look both spectroscopically and in images (e.g. Pinte et al. 2008; Eisner et al. 2005; Meixner et al. 2002; Men'shchikov et al. 2002; Voors et al. 2000; Sorrell 1990). RT modeling can be used to determine the effects of grain size distributions and mineralogy on the expected spectrum, and places constraints on the relative abundances of different grain types in a dust shell. However, optical functions used in such RT models must cover a broad wavelength range, from the ultraviolet (UV) to the infrared (IR). Deriving optical functions over this broad range requires laboratory transmission or reflectance spectra from multiple detectors; this is one of many reasons that $n, k$ are hard to find. As a result, various compilations have been produced that kluge to-

[1] Typical absorption spectra are derived from transmission experiments which yield the absorbance $a$ or the absorptivity $A$. The details of these different parameters and how they are derived are reviewed in Speck (2014).

[2] The complex refractive indices of a substance are often referred to as the "optical constants." Because these values are not constant, but rather vary with wavelength, temperature, and polytype (structure) as well as chemical composition of the sample, we use the term "optical functions" in this work.

[3] while RT models use absorption and scattering, or extinction efficiencies of candidate dust grains, many are equipped to use optical functions as inputs and do the conversion themselves, then generate the required cross-sections/efficiencies. Providing optical functions allows for more versatility in the modelling (e.g. grain size and shape effects)

gether observed and laboratory-collected data in order to produce optical functions to fill the full wavelength grid required by RT codes.

Still the most widely used optical functions for silicates are those from Draine & Lee (1984) (DL 1984, hereafter), Draine (1985, 2003) and Ossenkopf, Henning, & Mathis (1992) (OHM 1992, hereafter) which were originally generated 30 years ago and included kluges out of necessity. However, we are now able to provide optical functions which are kluge-free from the far-IR to the UV ($0.19 < \lambda < 250\,\mu$m). Here we present new laboratory-generated complex refractive indices for an iron-free glassy silicate of chondritic/solar atmospheric composition using a single sample for all wavelength regimes and compare it to the most commonly used "astronomical silicate" optical functions. We apply our new silicate glass optical functions to modeling the dust around HD 161796, an oxygen-rich pre-planetary nebula, in order to compare our new optical functions to those most commonly used. In addition we present new optical functions for metallic iron in order to properly model the relevant astrophysical environments.

There are a number of published laboratory datasets on metallic iron, (see also http://www.astro.spbu.ru/JPDOC/f-dbase.html), however, most have a very limited wavelength range. In astronomy, the most widely used data are from Ordal et al. (1988) which have both low resolution and do not extend to wavelengths shortward of the red-end of the visible spectrum. Pollack et al. (1994) also present a figure which contains a broad wavelength range optical function dataset for metallic iron, but this is compiled from multiple samples and thus not discussed further here. Likewise, there is a set of optical functions for metallic iron from Lynch & Hunter (1991) in Palik (1991), but it also is derived from a compilation of samples. Iron optical properties are also important for remote sensing in planetary science, but those studies are usually limited to the NUV–NIR range (see Cahill et al. 2012, whose own excellent data only covers 0.16–1.7 $\mu$m).

The new Fe optical functions improve upon the previous datasets because (a) most previous datasets do not extend beyond the red-end of the visible and (b) many are compilations from disparate samples. This leads to artifacts, such as a discontinuity in $R$ at 600 nm. In contrast, our new data has the higher spectral resolution, broader wavelength coverage, and is derived from the same sample through that wavelength range.

## 2. Past work: "Astronomical" and "circumstellar" silicates

Several different synthetic optical functions were derived at a time when there was insufficient laboratory data to be able to model astrophysical environments across a broad wavelength regime. A detailed discussion of lab data for Si-based materials can be found in Colangeli et al. (2003) as well as Speck et al. (2011), and a wider discussion of cosmic silicates can be found in Henning (2010). Speck et al. (2011) made detailed comparisons between previous published laboratory data on silicate glasses.

Compared to the wealth of data on potential astrominerals, our literature search (e.g. http://www.astro.spbu.ru/JPDOC/f-dbase.html Henning et al. 1999, and references therein) revealed that although silicates have been studied in more detail than other compounds, there are still shortcomings in the available data with respect to silicate glasses. Specifically, existing lab data on glasses do not allow astronomical spectra to be interpreted reliably in terms of either $M^{2+}$/Si or Mg/Fe ratio, which are important tools for discriminating between competing dust formation models (c.f. Speck et al. 2011, Figs. 7–9). Pitman et al. (2013b) compared the UV-Visible extinction coefficients (and imaginary index of refraction; $k$) for a range of silicates, both amorphous and crystalline with those from a variety of previously published samples. The figure from Pitman et al. (2013b) (reproduced in Fig. 1) illustrates that $k$ values vary wildly for both crystalline and amorphous silicates in the UV-vis, whether the datasets are from the lab or from modelers. The 70% and 80% Mg-rich silicate glasses of Dorschner et al. (1995), laser-ablated amorphous forsterite and enstatite from Scott & Duley (1996) and the "astronomical silicates" of DL (1984), OHM (1992), and David & Pegourie (1995) have a similar upper limit on $k$. The $k$ values for the remaining Dorschner et al. (1995) Mg-rich silicate glasses, sample 1-S from Jäger et al. (1994), and enstatite and olivine from Egan & Hilgeman

(1975a) are a factor of ten less. The datasets from Huffman (1975) are in a class by themselves (setting the uppermost limit on $k$), as are the Fe-rich silicate glasses. It is clear from that ostensibly similar compositions give rise to very different optical functions. In addition for crystallinity and composition differences, the variation in derived optical functions is also due to the use of powders, rather than bulk samples. Studis involving powder samples often overestimate the $k$ values because of internal reflections and scattering. This problem also afflicts bulk samples which include imperfections (see Hofmeister et al. 2009; Speck 2014; Speck, Hofmeister & Barlow 1999, for more detailed discussion of this issue.).

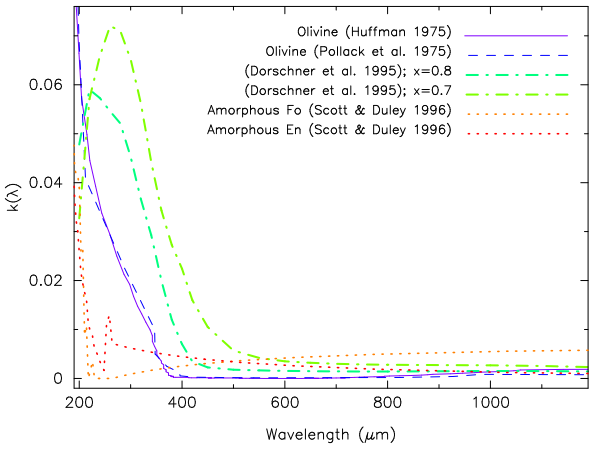


Fig. 1.— NUV–NIR Imaginary index of refraction, $k$, (a.k.a. extinction) of commonly used "Astronomical" silicates (reproduced from Pitman et al. 2013b)

Here we focus our discussion on the most commonly used datasets for analysis of silicate dust (DL 1984), Draine (1985, 2003) and OHM (1992). Other artificial "circumstellar," or "astronomical" silicates, based in part on real mineral data, also exist (Suh 1991; Laor & Draine 1993; David & Pegourie 1995). The optical functions in Suh (1991) were adopted from DL (1984) optical functions shortward of $\lambda = 8\,\mu$m and are thus not discussed here. David & Pegourie (1995) followed a similar methodology to DL (1984), but using the then new IRAS observations of ∼300 red supergiants. However, it is not widely used, probably because OHM (1992) had already supplanted DL (1984) for some purposes, and OHM (1992) incorporated the source data for David & Pegourie (1995) (from David & Papoular 1990) into their discussion. Laor & Draine (1993) is mostly based on DL (1984), but with tweaks at the high energy end ($>$ 20eV) which are calculated for an assumed density and $MgFeSiO_4$ composition, but these modifications were supplanted by Draine (2003) and not considered further here. Kim & Martin (1995) found a problem using DL (1984) to model UV polarization which they attributed to the use of crystalline olivine data in the derivation of "astronomical silicate" optical functions in DL (1984). Thus they proposed using measurements from volcanic glass in the UV to alleviate the problem. This is essentially still a kluge. In light of the above, in this work, we will focus on DL (1984); Draine (2003) and OHM (1992) datasets in our discussion.

Artificial "cosmic," "circumstellar," "interstellar," or "astronomical" silicate, optical and dielectric functions are not optimized at all wavelengths. For example, the "astronomical silicate" from DL (1984) is optimized for the mid-IR, but not in the UV-vis range (Pollack et al. 1994). Sorrell (1990) found that while DL (1984) "astronomical silicate" could produce a satisfactory match to the $10\,\mu$m feature in a protostellar object, it could not simultaneously match the UV region (c.f. Kim, Martin & Hendry 1994).

Synthetic "astronomical" or "circumstellar silicate" optical functions are often favored because they have broad wavelength coverage, especially at short wavelengths (UV and X-ray). As stated earlier, optical functions derived from merged laboratory spectra are collected piecemeal using multiple detectors; merging must be performed judiciously by the user. Furthermore, laboratory derived $n$ and $k$ values typically do not cover very far into the UV and X-ray range because these detectors must be hand built or, if commercially available, are very expensive. However, the trade-off in using synthetic "astronomical" or "circumstellar" silicate optical functions is that chemical composition has not been preserved across all wavelengths. The optical functions currently in widespread use were constructed by a combination of forward calculation from laboratory spectra of chemically disparate samples and backward calculation from astronomically-observed dust opacities, together

with pieces that are theoretically derived as illustrated in Figure 2. Those datasets also include modifications to specifically match certain astronomical observations. Consequently, whereas the synthetic optical functions match some interstellar spectra (in the case of DL 1984; Draine 2003) or circumstellar spectra (for OHM 1992), those $n$ and $k$ values are not useful for diagnosing changes from location to location and should not be used to interpret compositional effects. Indeed, DL (1984), Draine (2003), and OHM (1992) explicitly stated such caveats, but their warnings have been largely ignored because better alternatives have not been available.

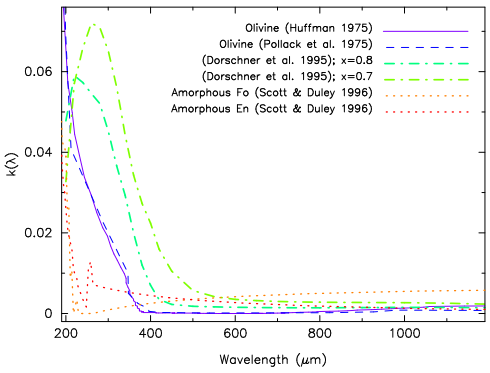


Fig. 2.— Source data for different wavelength regimes in previous "astronomical silicate" optical functions from DL (1984). Solid lines are the $n$ values. dashed lines are the $k$ values. These $n$ and $k$ are merged from a mix of experimental, observational, and theoretical data or assumptions. Main figure has linear axes: $x$-axis is wavelength in $\mu$m; $y$-axis is the value of the real or imaginary refractive index. Inset is the same as main figure but with log-log axes.

DL (1984)[4] produced synthetic optical functions for both "astronomical" silicate and graphite in order to model interstellar dust. Because of the paucity of laboratory data at that time, DL (1984) compiled data from multiple sources in order to achieve continuous wavelength coverage. The full procedure is described by Kim & Martin (1995) and summarized in Fig. 2

The updates by Draine (2003) apply mostly to the short wavelength/high energy end of the spectrum such that the values from DL (1984) were slightly modified: (1) a feature was removed at $\lambda^{-1} = 6.5\,\mu\mathrm{m}^{-1}$ ($0.15\,\mu$m); (2) for the sub-mm range ($250-1100\mu$m) the value of $\epsilon_2$ was varied by $\pm 12\%$ following Li & Draine (2001); (3) above 30 eV ($\lambda < 40$ nm) $\epsilon_2$ was estimated from atomic photo-absorption cross-sections, except near absorption edges. These high energy dielectric function values were merged with original functions from Draine (1985) between 18 and 30 eV ($40< \lambda <70$ nm).

OHM (1992) followed a similar method to that of DL (1984) and Draine (2003) but with different assumptions, constraints and observational data. In particular, OHM (1992) used an average of mid-IR observations from IRAS compiled by Volk & Kwok (1988). As in DL (1984) and Draine (2003), it was assumed that grains have an MRN grain-size distribution[5]. They also assumed a continuous distribution of ellipsoid shapes. For the NIR-MIR merge region, OHM (1992) used laboratory data from magnetite ($Fe_3O_4$) and metallic iron to get high enough opacities.

Both "astronomical" and "circumstellar" silicates will match some spectral features, and can be used for comparing optical depths between different dusty environments. However, because those $n$ and $k$ values are derived from a combination of laboratory and observed data as described above, they do not represent real solids across all wavelengths and thus cannot be used to determine the physical and chemical properties of dust in space, or how and why dust varies spatially or temporally. Moreover, because in the majority of systems, most light is absorbed and scattered in the NUV-NIR region, calculations of dust abundances are based primarily on optical properties for species that are expected to be rare ( e.g., crystalline olivine[6]) or are approximations (e.g., alumina/corundum $Al_2O_3$). In addition, because metallic iron is invoked either directly (in the case of OHM 1992) or indirectly (using "dirty silicates" in the case of Draine 2003), the effect of iron abundances on dust opacities cannot be determined with certainty. Because iron is predominantly gen-

[4]Electronic tables of the dielectric function ($\epsilon$) and equations to convert these to $n, k$ were published in Draine (1985).

[5]i.e., the number of grains of size $a$ is given by $n(a)$ proportional to $a^{-q}$, where $n$ is the number of the grains in the size interval $(a, a+da)$ and $q = 3.5$;$a_{min} = 0.005\mu$m; and $a_{max} = 0.25\mu$m (Mathis et. al 1977).

[6]based on the interpretation of observations

erated in Type Ia supernovae and the $\alpha$-rich silicon and magnesium atoms are predominantly made in core-collapse (Type II) supernova (Bulbul et al. 2012; Iwamoto et al. 1999; Nomoto et al. 2006), the relative abundances of these dust-forming elements may not scale together as we move from place to place, or especially back in time. The separation of iron is essential to understanding chemical evolution.

Finally, while optical functions do not depend on grain size/shape; the resulting absorption and scattering properties do. Consequently, the derivation of optical functions from (absorption and scattering) observations necessarily requires assumptions about the grains, in particular their size and shape distributions. For all the synthetic optical functions above, the grains are assumed to have MRN size distributions. Furthermore, DL (1984) and Draine (2003) assumed a specific form of oblate grains, while OHM (1992) assumed a broad continuous distribution of ellipsoids (including spheres, pancakes and needles).

## 3. Alternative: "cosmic silicate" glass

Here we present new optical functions for a "cosmic silicate" glass with chondritic/solar atmospheric abundances of the major elements excluding iron. These new optical functions were derived from laboratory spectra using the same sample of silicate glass from $\lambda$=0.19 to 250 $\mu$m. The composition is given in Table 1. As described in Speck et al. (2011), we excluded iron from the sample for two reasons: (1) to better preserve oxidation state; and (2) because several theoretical models of dust condensation suggest that iron does not commonly form silicates, but rather that it forms metallic iron grains (e.g., Lodders & Fegley 1999). Iron atoms are almost as common as magnesium and silicon atoms in the solar neighborhood, leading to some debate about the inclusion of iron in silicates. However, compositions that include grains that are agglomerations of iron-free silicates and metallic iron pieces are commonly invoked. Indeed, "dirty silicates" were suggested because iron-free silicates are too transparent (Merrill & Stein 1976).

In addition to our $n$ and $k$ for "cosmic silicate" glass, we also present $n$ and $k$ for metallic iron in order to demonstrate this opacity issue. Because our silicate is Fe-free, and we provide Fe optical functions, astrophysicists can now confidently investigate the effect of changing Mg/Fe abundance ratios in environments where dust forms. This is especially important in lower metallicity environments, where Mg/Fe should be higher than solar even though the absolute number density of atoms may be lower.

Table 1: Composition of "Cosmic Silicate" glass: $(Na_{0.11}Ca_{0.12}Mg_{1.86})(Al_{0.18}Si_{1.85})O_6$

| oxide | weight percent |
|---|---|
| $SiO_2$ | 54.26 |
| $Al_2O_3$ | 4.34 |
| MgO | 36.58 |
| CaO | 3.27 |
| $Na_2O$ | 1.61 |
| total | 100.05 |
| water content | ppm |
| $H_2O$ | 81 |

## 4. Experimental methods

### 4.1. Sample preparation

#### *4.1.1. Glass synthesis*

The sample studied here, "cosmic silicate," is an Fe-free silicate glass with chondritic/solar relative Mg, Al, Si, Ca, and Na abundances, synthesized as described by Getson & Whittington (2007) and Speck et al. (2011) by A. Whittington at the University of Missouri in Columbia. The melting and quenching techniques used produce more consistent, fully amorphized glasses than other sample preparation techniques (e.g., chemical vapor deposition, ion-irradiation, laser ablation; see discussion by Speck et al. 2011). The "cosmic silicate" glass is free of bubbles and internal crystals; electron microprobe composition from Speck et al. (2011) is given in Table 1.

Our "cosmic silicate" glass has a trace amount (81 ppm) of $H_2O$, and shows up as a very weak feature around 3 $\mu$m. For a binary, ternary, or quaternary silicate glass, we would expect to see at least one absorption in the range of 2.7 to 4.0 $\mu$m, depending on the composition of the glass (Brown & Martinsen 1972).

Given that $\epsilon'$ is proportional to constant $+10^{-22}$ times the concentration at long wavelengths (see e.g. Andeen, Schuele & Fontanella 1974), we can safely neglect the trace $H_2O$ amount in the IR.

#### *4.1.2. Metallic iron*

High purity electrolytic iron (>99.97%) was purchased from Alfa/Aesar®in the form of ∼cm-sized slabs with ∼mm thicknesses.

#### *4.1.3. Sample thickness determination*

We acquired spectral measurements of both the "cosmic silicate" glass and the metallic iron sample from polished slabs (in the UV-VIS-IR) and thin films (in the IR only). All polished slab samples were cut to sub-mm scale with a rock saw, then progressively ground, polished with micron-sized grits by hand, and (for transmission measurements in the IR) were thinned by compression in a diamond anvil cell to films of below 1 $\mu$m thick to achieve well-resolved spectral peaks and good signal-to-noise ratios in the spectra.

Many published papers and Bohren & Huffman (1983) suggest that grain shape has an effect on absorption and scattering cross-sections. Measuring optical properties from slabs, rather than loose or dispersed powders, ensures that the optical properties depend only on composition and not on grain shape or size. Also, using samples with differing thicknesses for different spectral segments helps to minimize the effect of back reflections (Hofmeister et al. 2009; Speck 2014).

For the thin films, the thickness of the film is the major driver of spectral quality. For the polished slabs, the quality of the laboratory spectra is affected by the quality of the sample's polish (for reflectivity) and the thickness of the sample (millimeter pathlength for reflectivity, lower limit of $\sim$40 $\mu$m achievable in the lab for transmission/absorption). We polished the slab samples to a surface roughness that is equivalent to that of the spectrometer's reference mirror for the IR instrument. In the UV, the high absorbance overwhelms the small effect of scattering from the surface.

The thickness of the sample, $L$, which factors into the determination of $k$, was measured for the polished slabs using a digital micrometer or a calibrated reticule in a doubly polished microscope. If spectral fringes were observed, we calculated the slab thickness from Eq. 1,

$$L = (2n_{vis}\Delta\nu)^{-1}, \quad (1)$$

where $\nu$ is frequency in cm$^{-1}$ and $n_{vis}$ is a tie-point for the real index of refraction in the visible. Our best determination of $n_{vis}$ of a thin (∼mm-scale), doubly polished slab of "cosmic silicate" glass using a gemological refractometer is 1.60±0.01, which is close to values for other glasses with like density. For the ultrathin slabs, interference fringes occur near the Christiansen minimum;[7] below, we use reflectivity data to compute $n$ and ultrathin slab thickness. For the thin films, because the fringes are in the transparent region when $n$ =1.6, we instead recorded the spacing of the diamond faces to estimate the film thickness. Spectra were aquired for an ultrathin slab with $L$ =38 $\mu$m, two thick slabs with $L$ =0.47 mm and 2.364 mm, and two micron-scale thin films. Using $n$ =1.6 gave 7.8 $\mu$m for the thick film and 3.5 $\mu$m for the thin film. Later spectral scaling suggests that $L$ =1.78 $\mu$m for the thinner film. The thicker of the two thin films was double the absorbance of the thin film, which is also consistent with the fringes.

### 4.2. Laboratory spectroscopy

We used several laboratory detectors at Washington University in St. Louis to measure room temperature (18–19°C) spectra across the UV-IR wavelength range. In the UV-VIS ($\lambda$ =190–1100 nm, $\lambda$ =0.19–1.1 $\mu$m, or $\nu$ =52,630–9090 cm$^{-1}$), we acquired unpolarized transmission and specular reflectivity spectra using the double-beam UV-1800 Shimadzu®UV-VIS Spectrophotometer to probe the mid-UV and the UV tail at high resolution (1 nm). The UV-VIS spectra were not acquired in an evacuated chamber.

The infrared spectrum for "cosmic silicate" glass was previously published in Speck et al. (2011). The same methodology from Speck et al. (2011) and Hofmeister (2003) was applied to measure the IR spectrum for metallic iron in this work.

[7] The Christiansen minimum occurs where the refractive index of a medium changes rapidly and may approach that of the surrounding medium (usually air or vacuum). This results in very little reflection or absorption (Conel 1969).

*4.2.1. Spectral merging*

For the "cosmic silicate" glass, spectral segments acquired for the two thin films, the ultrathin slab, and the two thick slabs were scaled in the region of wavelength overlap and merged. When scaling, the segment with the lowest absorbance was presumed correct. The lowest absorption that we can measure is the "noise" at the low point in $A$ near $\lambda = 2.5\,\mu$m ($4000\,\mathrm{cm}^{-1}$). We therefore shifted the spectrum up to avoid negative values; the smallest $A$ is 0.001 or 0.0001, consistent with the signal-to-noise ratio of the spectral segment. We scaled the thin film spectra to match the upturn at low frequency (high wavelength) for the slab sample. We used the data over the Si-O stretching peak for the thin film, but otherwise used the thick film. Spectra from the thick ($L \sim$0.47 mm) slab, rather than the ultrathin slab ($L \sim 38\,\mu$m), were used in the mid-IR due to noise considerations, although the data on the ultrathin slab were used to guide merging.

For the reflectance spectra, scaling was not necessary; spectra were merged so that the noise was minimized. For Fe, reflectivity is nearly 100% in the far-IR; attainment of this limiting value indicates that the absolute values were recorded. For the "cosmic silicate" glass, the reflectivity in the visible is in accord with independent measurements of $n$.

### 4.3. Optical function derivation

We derived the optical functions for both "cosmic silicate" and metallic iron which are shown in Figures 4 and 5.

For the metallic iron spectra, we performed Kramers-Kronig analysis on the reflectivity data to obtain $n$ and $k$. For details, see e.g., Spitzer et al. (1962); Andermann, Caron & Dons (1965) However, applying the standard methods for our "cosmic silicate" was problematic. Reflectivity $R$ for Mg-Ca-Si-O glasses is low (20% at the peaks, compared to ∼80% for crystalline silicates with similar composition; c.f. Merzbacher & White 1988). Consequently, the standard methods used to derive $n$ and $k$ for crystalline silicates sometimes fail to provide positive values for the dielectric function $\epsilon_2$ at all $\lambda$ for amorphous or glassy silicates. This problem can be understood in terms of glass structures. Specifically, classical dispersion (damped harmonic oscillator model) assumes that the spectral peak breadths are due to damping (mode interactions), but in glasses, peak breadths also arise from a continuum of bond lengths in the glass and multiple overlapping peaks in the spectrum. Likewise, Kramers-Kronig analysis fails to produce physically reasonable values when peaks are unresolved doublets (Giesting & Hofmeister 2002).

We use an alternative, more direct method to derive $n$ and $k$ values for our "cosmic silicate" glass. Using absorption, reflectivity, and sample thickness, we determine the imaginary index of refraction $k(\lambda)$ via Eqs. 2–4 and then use our reflectivity spectra $R$ to calculate $n(\lambda)$ using Eqs. 4–5.

At all $\lambda$, $k$ was determined from absorption data where we corrected for reflections. Let $\frac{I_{trans}}{I_0} \equiv$ transmittance, such that lab absorbance, in common logs is represented by Eq. 2,

$$a_{SCM} = -log_{10}(I_{trans}/I_0). \quad (2)$$

For the polished slabs, we assumed that the measurement includes back reflections ($R$) from the slab's top and bottom faces and compute the true or ideal absorption coefficient ($A$) after Hofmeister et al. (2009) and Speck (2014),

$$A = 2.3026[a_{SCM} + 2log_{10}(1 - R)]/L. \quad (3)$$

For the "cosmic silicate" glass, Eq. 3 overcorrects because the reflection from the back surface of the sample is less than $R$ due to light being attenuated slightly. Thus, we adjusted the spectra manually for this effect and set $R = 0$ in Eq. 3 for the "cosmic silicate" glass. We then calculated the imaginary part of the complex refractive index $k$ using Eq. 4:

$$k_\lambda = \frac{A}{4\pi\nu}. \quad (4)$$

The value of $k$ is fixed at 0 for $\nu$ =0 $\mathrm{cm}^{-1}$ and for very large $\nu$ above the X-ray region.

Laboratory reflectivity ($R$) equals $\frac{I_{meas}}{I_0}$. Iron-free glasses are very transparent and $R$ is thus very low in the near-IR to visible; in this range, we computed $R$ from Fresnel's relationship, Eq. 5,

$$R = [(n-1)^2 + k^2][(n+1)^2 + k^2], \quad (5)$$

using measured $n_{vis}$ and $k$ =0. At other wavelengths, we invert Eq. 5 to provide $n(\lambda)$ from measured $R$ and $k$ (Eq. 6):

$$n(\lambda) = \frac{1+R}{1-R} + \sqrt{-1-k^2+(\frac{1+R}{1-R})^2} \qquad (6)$$

For metallic iron, our $n$ and $k$ values extend to at $\lambda$ =0.19 $\mu$m; we did not extrapolate to shorter wavelengths. All metals have nearly 100% reflectivity in the far-IR, which arises from the nearly free electron model of Drude (1900) as discussed in Wooten (1972).

For the "cosmic silicate" glass, because the composition was nearly 1 MgO + 1 $SiO_2$, $n$ and $k$ were averaged from data on MgO and silica glass in Palik (1985). Also, $n$ is pinned at unity above the X-ray region and $k$ goes to 0 at very short wavelength. At long wavelengths (far-IR), we assumed that $k$ decreases to $10^{-7}$ at 0.001 $cm^{-1}$ (10 m and that $n$ asymptotes to 3.16 at 0.001 $cm^{-1}$ The value of $k$ is an estimate, based on the value of $k$ approaching 0 as the frequency goes to zero. The value of $n$ is from the low frequency dielectric function, calculated below.

According to Appen & Bresker (1952), the dielectric constant is additive and can be estimated from the oxides using:

$$\epsilon = \Sigma \epsilon_i p_i$$

where $p_i$ is the fraction of the i$^{th}$ component and $\epsilon_i$ was obtained at 0.45 GHz (0.015 $cm^{-1}$) from the table in Appen & Bresker (1952). See also the table on p. 318 of Scholze (1991)[8].

## 5. Comparing optical functions

Our new optical functions for "cosmic silicate" glass and metallic iron are compared to popular optical functions currently in use, i.e., Draine (2003) for silicate and Ordal et al. (1988) for metallic iron in Figures 4 and 5. Figure 4 clearly demonstrates that at $\lambda > 0.2\,\mu$m the differences are huge. In particular, the imaginary part of the complex refractive index ($k$) is several

[8]also available here: http://www.lehigh.edu/imi/docs_GP/Slides/GlassProp_Lecture22_Jain1.pdf page 24

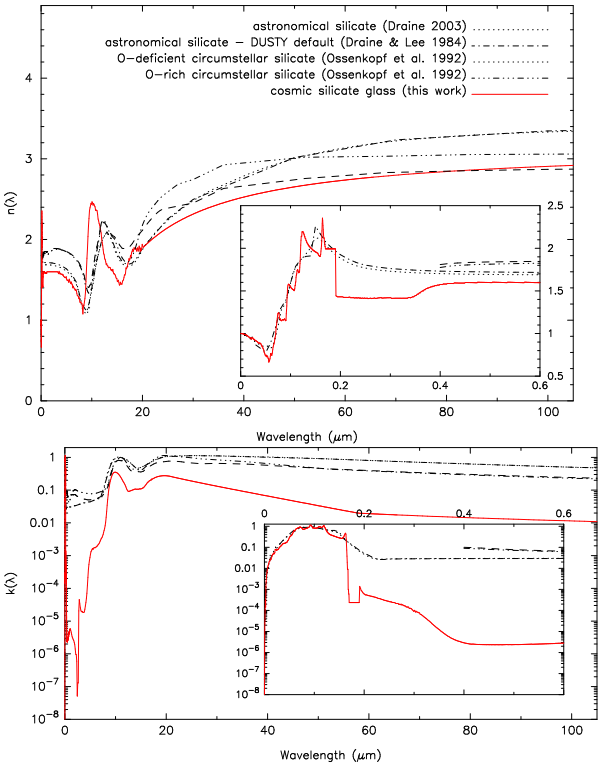


Fig. 3.— Comparison of complex refractive indices ($n$ & $k$) for "Cosmic" and "Astronomical" silicates. Solid line ≡ this work; dotted and dashed lines ≡ past works. *Insets* are close-up views of the UV-vis region; *Top*: real part of complex refractive index; *Bottom*: imaginary part of complex refractive index; $x$-axis is wavelength in $\mu$m.

orders of magnitude lower in our new "cosmic silicate" glass measurements than in those derived by Draine (2003). In part this difference comes from the difference in methods. The new data are determined from experimental laboratory data whereas the Draine (2003) data are interpolated in this region and were specifically fixed to get high enough opacity to match observations.

Figure 5 shows that our new optical functions for metallic iron match the overall strength and shape of the data from Ordal et al. (1988). However, our higher resolution spectroscopy measurements reveal details with the optical properties of metallic iron not seen in the Ordal data. In particular the real part of the refractive index ($n$) drops to a very low value at $\lambda$ ∼20 $\mu$m and ∼50 $\mu$m; meanwhile, the imaginary part, $k$, shows a bump

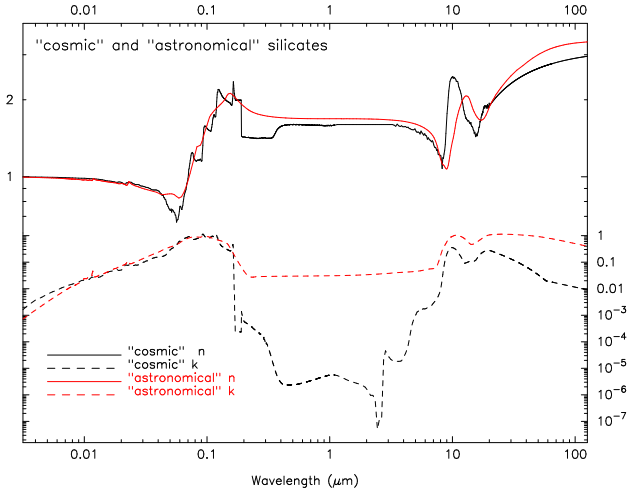


Fig. 4.— New optical functions of "cosmic silicate" glass from this work (black lines), compared to "astronomical silicate" from Draine (red lines 2003).

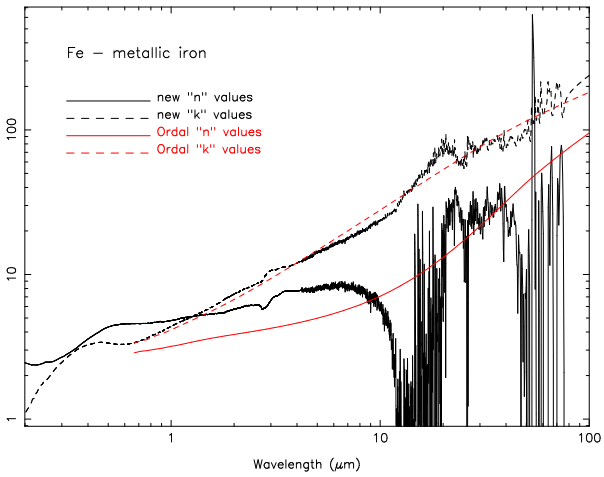


Fig. 5.— New optical functions of metallic iron from this work (black lines), compared to values from Ordal et al. (1988) (red lines).

around 30 $\mu$m. In addition, the new optical functions extend down into the UV-Visible part of the spectrum, rather than ending at the NIR/visible boundary. This is very important for modeling in the interstellar medium or stars above about K type, because the majority of the flux is emitted in this higher energy region.

Our values differ from and better represent Fe than those of Ordal et al. (1988) for the following reasons. The tables of $n$ and $k$ in Ordal et al. (1988) are widely spaced (by 20 cm$^{-1}$) in the far-IR; the spacing is even greater at shorter wavelengths. Also, the Ordal et al. (1988) data were obtained from a Kramers-Kronig analysis that incorporated a Drude (1900) model at high and low frequencies (short and long wavelengths). We did not use a Drude model. Kramers-Kronig analysis is effectively a smoothing function; this smoothing, combined with their low resolution, makes the Ordal et al. (1988) $n$ and $k$ data very smooth and prohibits resolution of narrow features. Our high-resolution iron data resolve the narrow features. In the visible, we also see a feature at ~0.4–0.5 $\mu$m in our $n$ and $k$ data that was observed in previous studies (see e.g. Palik 1991) with a discontinuity between their non-overlapping data sets. Our data are continuous across this feature and so improve upon these past works. In the near-IR, the small feature at 2–3 $\mu$m in our iron data is not an artifact and is observed due to our high instrumental resolution. Therefore, we have provided improved $n$ and $k$ at higher resolution. The trade off is the noise in the far-IR longer than 10 $\mu$m; however, as will be seen in § 6 this noise does not affect our radiative transfer models of the observations.

## 6. Radiative transfer modeling

### 6.1. *DUSTY*

We used the 1-D radiative transfer program *DUSTY* (Ivezic & Elitzur 1995; Nenkova et al. 2000) to determine how our new "cosmic silicate" glass optical functions perform against previous "astronomical" and "circumstellar" silicates $n$ and $k$. For our test case, we built simple models for HD 161796, a dusty oxygen-rich pre-planetary nebula/post asymptotic giant branch star. We chose HD 161796 for several reasons: (1) it has been observed many times over several decades and over a large wavelength range, and thus has a well sampled spectral energy distribution (SED), as shown in Figure 6; (2) its central star is hot enough to emit significant UV radiation, but not so hot that photo-dissociation and ionization play a major role in the nebula, simplifying the modeling; and (3) although not completely spherical, it is a remarkably round object (Ueta et al. 1999) and thus using a 1-d RT code is a reasonable approximation.

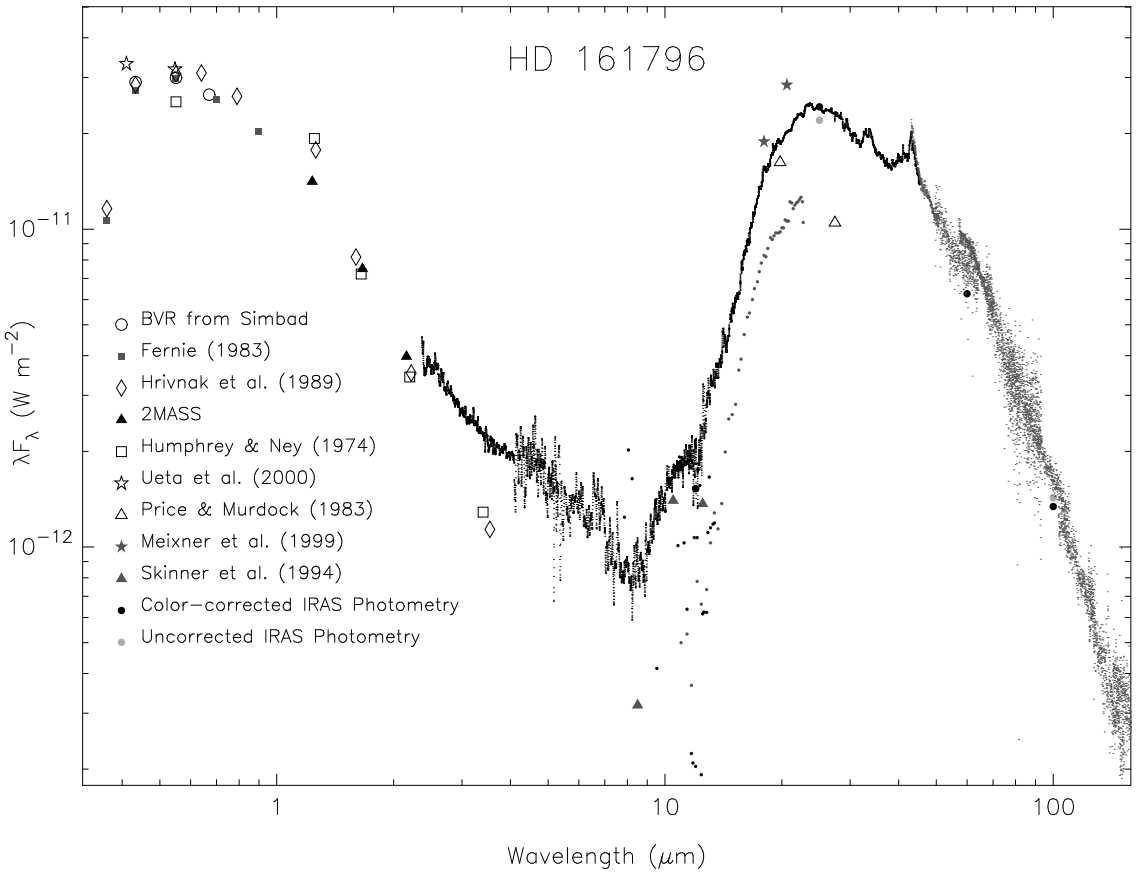


Fig. 6.— Spectral Energy Distribution (SED) of HD 161796. Very small black dots are the *ISO* SWS data; very small grey dots are the *ISO* LWS data; medium black filled circles are the short wavelength *IRAS* LRS data; medium grey filled circles are the long wavelength *IRAS* LRS data; large filled circles are the *IRAS* photometry data (grey are uncorrected; black are color corrected). Sources for other photometry points are given in the legend. $x$-axis is wavelength in microns; $y$-axis is flux ($\lambda\, F_\lambda$) in $\mathrm{W\,m^{-2}}$.

### 6.2. Modeling HD 161796 with synthetic optical functions

We have generated models using the new "cosmic silicate" glass $n, k$ data presented herein as well as using synthetic optical functions from Draine (2003); DL (1984); OHM (1992), which are compared in Fig. 7.

For our models we adopt the central star temperature, $T_\star = 6750\,\mathrm{K}$, from Hoozgaad et al. (2002), which falls within the currently acceptable range for the object's central F3Ib class star (6699 K, 6600 K, 6700 K, 6900–7350 K; Koytyukh 2007; Lyubimkov et al. 2010; Lang 1992, respectively) and previous models (Skinner et al. 1994; Meixner et al. 2002). Fig. 7 shows that the effect of varying this $T_\star$ value by $\pm 150\,\mathrm{K}$ is negligible (c.f. DePew et al. 2006). DUSTY and many other RT models invoke Mie theory to calculate absorption and scattering cross-sections when a user supplies $n$ and $k$. The simple models shown here are made with the default DUSTY settings, which implicitly assume separate populations of spherical grains. However, spherical grains are probably inappropriate in many astrophysical environments and are not the best representation of silicate features or of metals, whose FIR behavior is extremely shape and agglomeration dependent. For "real" models, we recommend supplying absorption and scattering coefficients for non-spherical grains calculated directly from $n$ and $k$. In that way, our new $n$ and $k$ values allow users to in-

vestigate the effect of grain size and shape (e.g. Pollack et al. 1994; Min et al. 2003).

Figure 7 (*top*) shows the effect of using the best-fitting model for the Draine (2003) function model with the original "astronomical silicate" from DL (1984), and with the warm and cold "circumstellar silicate" optical functions from OHM (1992). Figure 7 (*bottom*) shows the best-fitting models using the original "astronomical silicate" optical functions from DL (1984) and those from OHM (1992), all three of which are embedded options in *DUSTY*. All model parameters are shown in Table 2. The difference in performance between DL (1984) and Draine (2003) is that the V-band optical depth is very slightly lower when using the newer Draine (2003) optical function. Using the OHM (1992) synthetic functions requires even lower V-band optical depths.

We assumed a radial dust density distribution of $\frac{1}{r^2}$ to reflect a constant mass-loss rate. We also initially assumed that the outer radius of the dust shell ($R_{\rm out}$) is $100\times$ the inner radius ($R_{\rm in}$), although the models are not very senesitive to this parameter. Speck et al. (2009, and references therein) demonstrated that the inherent degeneracy in RT modeling means that this number can be changed by compensating using the inner dust radius/temperature. Therefore we arbitrarily chose this value for comparison purposes. We used an MRN grain-size distribution to be consistent with the assumptions of Draine (2003); DL (1984); OHM (1992). Speck et al. (2009) showed that *DUSTY* models of spectral energy distributions are not very sensitive to the precise grains size distribution as long as the distribution does not exclude many small grains or include very big grains ($>1\,\mu$m).

Table 2: Best-fitting *DUSTY* models using synthetic optical functions from DL (1984); Draine (2003); OHM (1992)

| source | $\tau_V$ | $T_{in}$ |
|---|---|---|
| D2003 | 2.25 | 125 |
| DL84 | 2.35 | 125 |
| OHM92-C | 1.75 | 125 |
| OHM92-W | 1.75 | 115 |

### 6.3. Modeling HD 161796 with our new "cosmic silicate" optical functions

Our purpose in developing these simple models (an example of which is shown in Fig. 8) is not to make an exhaustive study of the parameter space, or to optimize the fit to this particular object's SED, but instead to demonstrate the effect of using the new, real mineral data presented herein compared to more commonly use "synthetic" complex refractive indices. We have deliberately chosen the minimum number of dust components necessary for a fit and commonly used model parameters such as the $\frac{1}{r^2}$ radial density distribution and the MRN grain-size distribution with spherical grains. The effect on radiative transfer modeling of choosing other parameters is discussed by Speck et al. (2009).

#### *6.3.1. "Cosmic silicate" ONLY*

The initial models assumed a single dust component; later models included metallic iron and "cosmic silicate". We also included external heating of the dust shell by the interstellar radiation field as well as a pile-up of material in the outer regions of the dust shell where the stellar outflow meets the interstellar medium in order to investigate whether composition or other factors improve the match to the shape of the SED (c.f. Gillett et al. 1986; Young, Phillips & Knapp 1993).

Models using only our new "cosmic silicate" glass optical functions do not match the data or the models using synthetic optical functions. There are two issues: (1) The shape of the SED produced using "cosmic silicate" is too symmetric and cannot match the observed emission at far-IR wavelengths; and (2) the visual optical depth required is unfeasibly high ($100 < \tau_V < 150$). We investigated the effect of varying several model parameters in an attempt to alleviate the far-IR problem including the radial density distribution, the geometrical size of the dust shell, inclusion of crystalline silicates, inclusion of a step function in the density distribution to replicate the potential pile-up where the circumstellar materials meet the ISM, and inclusion of external heating of the dust shell by the interstellar radiation field (see, e.g., Gillett et al. 1986; Young, Phillips & Knapp 1993). None of these resolved either problem with

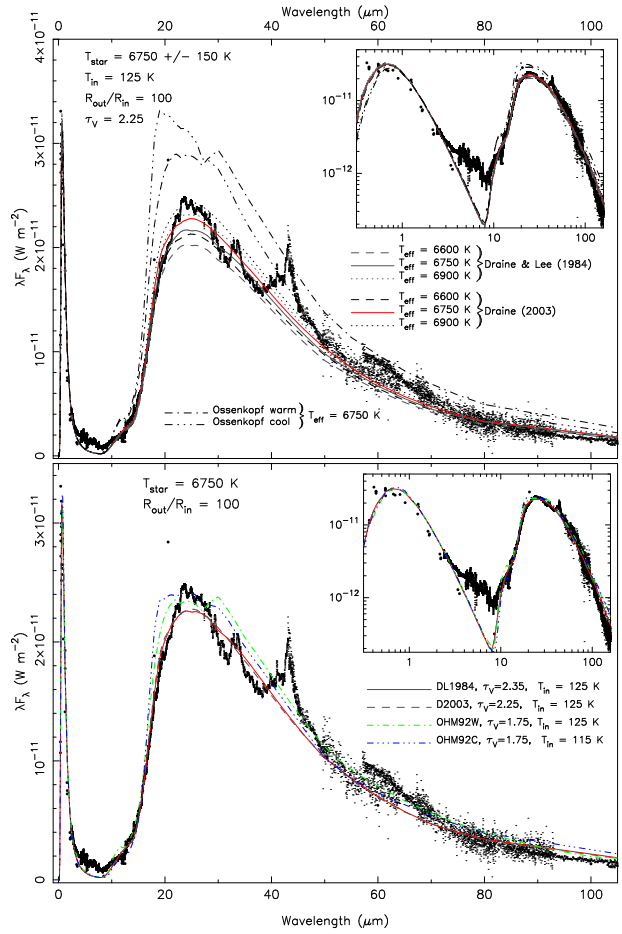


Fig. 7.— Best-fitting *DUSTY* models for "Astronomical Silicate". $x$-axis is wavelength in microns; $y$-axis is flux ($\lambda F_\lambda$) in $\mathrm{W\,m^{-2}}$. Main panel is a linear-linear plot; inset is a log-log plot of the same data. In all panels, large black filled circles = photometry points from Figure 1; very small dots = *ISO* spectrum. *Top*: Best model fit is achieved using complex refractive index from Draine (2003). The effect of varying $T_\star$ by ±150K is negligible. *Bottom*: Best-fitting *DUSTY* models using complex refractive index from Draine; DL; OHM for $T_{star}$ =6750K and varying opacities.

the "cosmic silicate" only models.

### 6.3.2. *"Cosmic silicate" and metallic iron models*

As discussed above (§ 2), grains containing a mixture of metallic iron and iron-free silicates have long been invoked to account for the low opacity of silicates either explicitly (e.g. Merrill & Stein 1976; OHM 1992) or implicitly (e.g. Draine 2003, and references therein). Condensation models suggest that iron should form as metallic iron grains rather than as part of a solid solution of ferromagnesian silicates (e.g. Lodders & Fegley 1999). Therefore we also included metallic iron grains into our models, along with "cosmic silicate" glass, in varying proportions. DUSTY assumes that the grains are co-spatial; i.e. the absorption and scattering cross-sections are calculated assuming the different grain compositions have the same size distribution and have the same temperature (essentially it a composite grain, comprising a silicate sphere and an iron sphere in thermal contact.)

Figure 8 shows that a modest addition of metallic iron dramatically improves both the shape and the optical depth requirements for the models. With only 25% metallic iron grains, we can reduce the optical depth to ∼2, comparable to the models with synthetic optical functions.

Whereas including iron into the models improves the values for the visual optical depth, we still have a modeled SED that is narrower than either the observations or the models using synthetic optical functions. Inclusion of crystalline silicates (which are obviously present based on the *ISO* spectrum in Fig. 6 and have been included in previous models, e.g. Hoozgaad et al. 2002) also does not alleviate the problem of SED shape and produces short wavelength crystalline features not seen in the observational data.

### 6.3.3. *Two-layer models*

Consequently, we used *DUSTY* to build a 2-layered model, which is shown schematically in Fig. 9. The inner part of the shell is modeled to get the best fit shortward of 35 $\mu$m. The output from this model is then the inner central source for the second layer model. Because RT modeling is inherently degenerate, there are several models that produce good fits, summarized in Fig 9. All good fits consist of an inner region dominated by "cosmic silicate" glass, with 25% metallic iron, and a geometrically thin outer zone where the composition no longer contains any glassy silicate. Instead the thin outer layer contains 10% metallic iron, 30% Fe-rich pyroxene from Henning & Mutschke (bronzite; 1997) and 60% forsterite (from Pitman et al. 2013a).

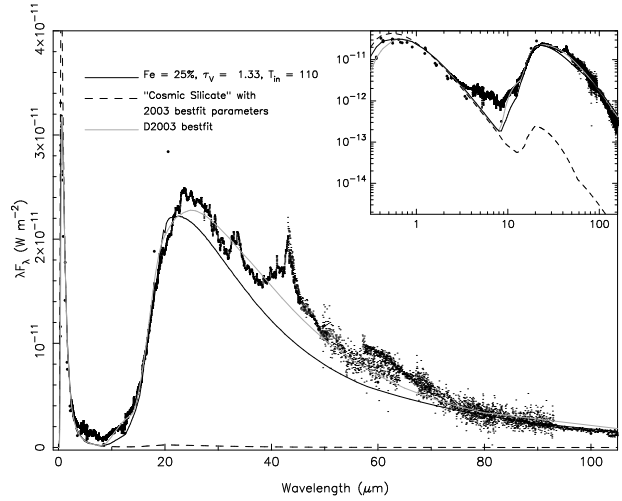


Fig. 8.— Best-fitting *DUSTY* models for "cosmic silicate" with metallic iron included. $x$-axis is wavelength in microns; $y$-axis is flux ($\lambda\, F_\lambda$) in $\mathrm{W\,m^{-2}}$. Main panel is a linear-linear plot; inset is a log-log plot of the same data. In both panels, large black filled circles = photometry points from Figure 1; very small dots = *ISO* spectrum. Thin black dashed line = model with "cosmic silicate" $n$ & $k$ from this work, but Draine (2003) best-fitting model parameters; thin grey solid line = best-fitting model using Draine (2003); thick black solid line = best-fitting using "cosmic silicate" $n$ & $k$ with 10% metallic iron; thick black dotted line = best-fitting using "cosmic silicate" $n$ & $k$ with 20% metallic iron.

Henning & Mutschke (1997) do not state whether the iron (FeO) content is given as mole % or weight%. However, in either case the sample should be referred to as Fe-rich enstatite rather than bronzite. We use this mineral as an example of a single crystalline silicate, rather than an attempt to match all the features. The best 2 layer model is shown in Fig. 10.

This model may suggest that crystallization of silicates occurs either as a result of shock heating of grains where the circumstellar medium ploughs into the surrounding ISM; or as a result of high energy (FUV) photons coming from the ISRF. It is possible that this thin layer is also where many of the silicate grains are destroyed, which would account for the difference between circumstellar and interstellar silicate features. Indeed, it has been posited that most interstellar silicates form in cold, dark molecular clouds rather than being ejected from dying stars (e.g., Zhukovska 2008; Draine 2009). However, this idea is controversial (see, e.g. Jones & Nuth 2011).

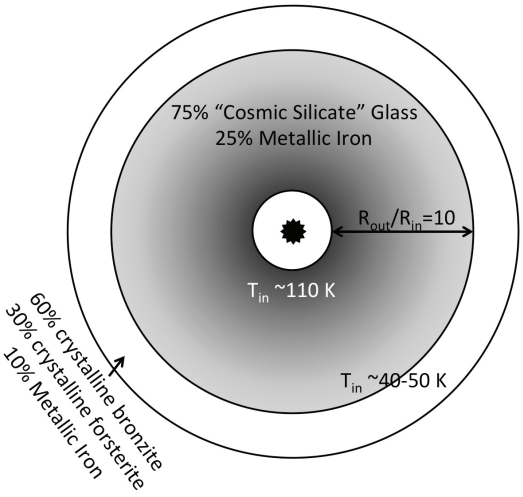


Fig. 9.— Schematic cartoon of the 2-layer *DUSTY* models

### 6.4. Iron optical functions

There is a subtle effect as a result of replacing the widely used metallic iron optical functions from Ordal et al. (1988) with our new metallic iron optical functions. In order to match the model using the Ordal et al. (1988) data we had to either increase the visual optical depth or increase the fractional abundance of metallic iron in the model.

## 7. Discussion

It is clear from the way in which the optical functions for "astronomical silicates" were derived that they have some limitations. At the short wavelength end, the materials used do not actually represent the solids we expect to be dominating astrophysical environments. At the long-wavelength end, the data are derived from astronomical observations and assumptions and thus provide no flexibility to match environments with different dust components. Past attempts to derive the optical functions for astrophysically-relevant silicates were hampered by the lack of availablity of consistent laboratory data at that time. Decades later,

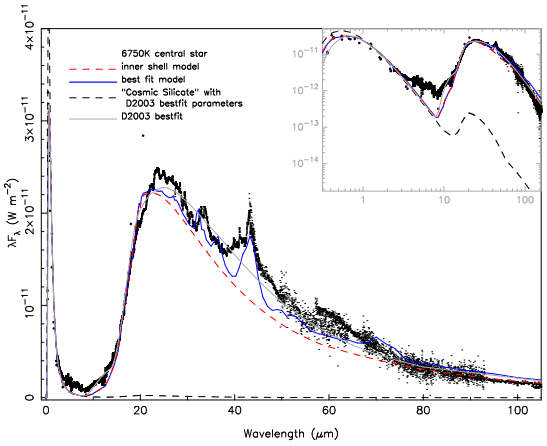


Fig. 10.— Best-fitting *DUSTY* models using two-layer approach. $x$-axis is wavelength in microns; $y$-axis is flux ($\lambda F_\lambda$) in $\mathrm{W\,m^{-2}}$. Main panel is a linear-linear plot; inset is a log-log plot of the same data. In both panels, large black filled circles = photometry points from Figure 6; very small dots = *ISO* spectrum. Thin black dashed line = model with cosmic silicate $n$ & $k$, and Draine (2003) best-fitting model parameters; thin grey solid line = best-fitting model using Draine (2003); thin red dotted line = inner shell model thick blue solid line = 2-layer model = inner model with thin shell of crystalline silicate and metallic iron on the outside. See schematic cartoon in Fig 9.

we now have the means to overcome at least some of these issues.

The 10 $\mu$m silicate feature occurs in many dusty astrophysical environments. It varies from object to object and even within a single object both temporally (e.g., Monnier et al. 1998; Guha Niyogi et al. 2011a) and spatially (e.g., in $\eta$ Car, N. Smith, Pers. Comm; and Guha Niyogi, Speck & Volk 2011b). Within a single type of astrophysical object, the feature shows huge variations in terms of its peak position, width and its ratio to the $\sim$ 18$\mu$m feature (e.g., Speck 1998; OHM 1992). Variations in feature or SED shape from object to object cannot be analyzed modeling with synthetic optical functions.

Small circumstellar dust particles are likely much more compositionally and structurally inhomogeneous than the simple glass + Fe cases we have considered here. Thus, we are providing data on well-characterized endmember glass to allow modelers to mix different compositions and impurities as they choose. Our data also can aid in distinguishing between dust that is glassy, crystalline, or some combination of the two, which is important because the degree of structural homogeneity has implications for its formation, and subsequent processing, evolution and destruction (Speck et al. 2011).

### 7.1. Comparison to previous models

HD 161796 is a well-studied object and many previous models exist, which makes it an excellent test case. Hrivnak et al. (1989) produced models of several candidate pre-planetary nebulae, including HD 161796, using dust opacities derived from Volk & Kwok (1988). Their output parameters depend on distance, but are consistent with the later models in terms of inner dust radius and stellar luminosity.

Justtanont et al. (1992) made a very simple model of HD 161796's SED using a 6000 $L_\odot$ F-type star surround by dust with a single blackbody at 90 K modified by the emissivity from disordered olivine from Krätschmer & Huffman (1979) and assuming an MRN size distribution. Their best-fitting model did not match the SED at all wavelengths, and although it was somewhat improved by the addition of magnetite, there remained mismatches between the model and the observed SED.

Skinner et al. (1994) used multiwavelength imaging to constrain their models of HD 161796. Their model assumed an effective star temperature of 6300 K and used astronomical silicate from DL (1984) in an MRN distribution. Their best-fitting model gave a stellar luminosity of 3600Ł$_\odot$ and an inner dust radius of $8.9\times10^{15}$ cm.

Up to this point, the past models assumed spherical symmetry (as do we). Furthermore, there was not yet observational evidence for crystalline silicates. With the advent of *ISO*, more detail in the far-IR spectrum was revealed and led to modeling including crystalline silicates. Hoozgaad et al. (2002) modelled the full 2–200 $\mu$m *ISO* SWS + LWS spectrum together with additional data extending the SED from the optical to the millimeter wavelength range. Their model assumed a star of 3000Ł$_\odot$ at 6750 K with an inner dust radius of $21\times10^{15}$ cm (and outer radius of

$63\times10^{15}$ cm). Hoozgaad et al. (2002) developed a two layer model in which the inner dust is dominated by amorphous silicate and the outer dust includes a mantle of water ice. They used a number of different optical functions in their model in order to cover the full wavelength range, but the amorphous silicate was solely from OHM (1992) and was extrapolated out to the extremes of the wavelength range. In addition, they included crystalline water ice, as well as crystalline silicates in the form of enstatite and forsterite. They focussed on developing two parts of their model - the core-mantle grains and the crystalline silicate fraction, although they found that the lack of sensitivity of the models to the precise abundances of crystalline silicates made abundance constraints weak, but found that ∼10% by mass was reasonable. The average temperature for the amorphous silicate grains was found to be 110 K (and ranged from 47–137 K) while the crystalline grains were cooler (at ∼50-90 K), consistent with our results.

Meixner et al. (2002) produced a 2-d model of HD 161796 for which they combined both multiwavelength imaging and the SED to constrain their models. Their best-fitting model had a $2800 L_{\odot}$ star with an effective temperature of 7000 K. They found an inner dust temperature of 110 K and a corresponding inner dust radius of $11\times10^{15}$ cm. Whereas the model is axisymmetric, the change in dust density from equator to pole is small. Their model included both forsterite and enstatite but the coarse spectral resolution precluded fitting the narrow crystalline silicate features in detail. The grain size distribution is KMH-like with a higher upper limit on grain size, and they assumed the dust composition from Hoozgaad et al. (2002).

Given the range of optical functions and model types used, it is interesting (and reassuring) that all models including ours end up being dominated by amorphous silicate dust at ∼100 K. However, previous models used synthetic optical functions for amorphous silicates and thus did not include the correct Fe/Mg fraction and cannot reveal the shell structure seen in our modeling results.

## 8. Conclusions

We have presented new optical functions for iron-free glassy silicate with chondritic composition and metallic iron, extending from UV to far-IR wavelengths (0.19-250 $\mu$m), which are measured directly in the laboratory using the same sample throughout. The "cosmic silicate" data extend to the X-ray region. These new optical functions improve upon prior synthetic optical functions for "astronomical" and "circumstellar" silicates by preserving the chemical composition, sample properties and the method of optical function derivation (all lab data). A simple model excursion using HD 161796 as an example shows that:

1. using synthetic optical functions automatically fits most SED slopes and thus provides false parameters for models.

2. inserting back-calculated $n$ and $k$ from observed data is not necessary to achieve the desired SED slope; only a small amount of metallic iron is needed to make the models sufficiently opaque;

3. the precise ratio of iron/cosmic silicate strongly affects the far-IR emissivity law. Thus, our new laboratory-derived optical functions can be used to determine how composition affects observed long-wavelength emissivities and emissivity indices ($\beta$ value), which is relevant to understanding many long wavelength observations including those from *ALMA* and *Herschel*, *Spitzer*, *IRAS* and *ISO*;

4. our models of HD 161796 hints at crystallization of silicates at the outer edge of the circumstellar shells. While this is a preliminary result that requires further study, this suggestion is not apparent when using synthetic optical functions;

Because our cosmic silicate has chondritic abundance, it may not be precisely the composition of glassy silicates formed away from the solar neighborhood. Future work will include other silicate glass compositions including both iron-free and iron-bearing compositions.

This material is based upon work supported by the National Science Foundation under Grant

No. AST 1009544. The authors thank A. Buffard for preliminary *DUSTY* models, A. Whittington for producing the synthetic glass samples and A. Corman & J. Goldsand for laboratory assistance. Electronic tables of the spectra shown in this work are available as an electronic supplement to this article and at `http://galena.wustl.edu/$\sim$dustspec/idals.html`.

## REFERENCES

Andeen, C., Schuele, D., Fontanella, J., 1974, J. Appl. Phys. 45, 1071

Andermann, G.; Caron, A.; Dows, David A., 1965, J. Opt. Soc. Am. 55, 1210.

Appen, A. A., Bresker, F., 1952, J. Techn. Phys. 22, 946

Aurière, M. 1982, A&A, 109, 301

Bohren, C. F., Huffman, D.R., 1983 "Absorption and Scattering of Light by Small Particles", Wiley, New York

Bouwman, J., Meeus, G., de Koter, A., Hony, S., Dominik, C., Waters, L. B. F. M. 2001, A&A, 375, 950.

Brown, L. E., W. E. Martinsen. 1972, Proceedings of the Oklahoma Academy of Science, 52, 143.

Bulbul, Esra, Smith, Randall K., Loewenstein, Michael, 2012, ApJ, 753, 54.

Cahill, J. T. S., D. T. Blewett, N. V. Nguyen, K. Xu, O. A. Kirillov, S. J. Lawrence, B. W. Denevi, and E. I. Coman 2012, Geophys Res Lett, 39(L10204).

Cahill, J. T. S., D.T. Blewett, N. V. Nguyen, and S. J. Lawrence, 2015, Icarus, in preparation.

Colangeli, L., Henning, Th., Brucato, J. R., Clment, D., Fabian, D., et al., 2003, A&ARv, 11, 97.

Conel, J.E., 1969, J. Geophys. Res., 74, 1614.

David, P. Pegourie, B. 1995, A&A, 293, 833.

David, P., Papoular, R. 1990, A&A, 237, 425.

DePew, K., Speck, A., Dijkstra, C., 2006, ApJ, 640, 971.

Dorschner, J., Begemann, B., Henning, T., Jaeger, C., Mutschke, H. 1995, A&A, 300, 503.

Draine, B. T. 2009, In proceedings of *Cosmic Dust - Near and Far* ASP Conference Series, Vol. 414, Edited by Thomas Henning, Eberhard Grn, and Jrgen Steinacker. San Francisco: Astromomical Society of the Pacific, p.453.

Draine, B. T. 2003, ApJ, 598, 1017.

Draine, B.T., 1985, ApJS, 57, 587.

Draine, B. T., Lee, H. M. 1984, ApJ, 285, 89.

Drude, P., 1900, Annalen der Physik 1, 566; 3, 369.

Egan, W. G., Hilgeman, T., 1975, AJ, 80, 587.

Egan, W. G., Hilgeman, T., 1975, Icarus, 25, 344.

Eisner, J. A., Hillenbrand, L. A., Carpenter, John M., Wolf, S. 2005, ApJ, 635, 396.

Forrest, W. J.; McCarthy, J. F.; Houck, J. R., 1979, ApJ, 233, 611.

Getson, J.M., Whittington, A.G. 2007Journal of Geophysical Research, 112, B10203,

Giesting P.A., Hofmeister A.M. 2002, Physical Review B, 65, Issue 14, id. 144305.

Gillett, F.C., Backman, D.E., Beichman, C., Neugebauer, G., 1986, ApJ, 310, 842.

Guha Niyogi, S., Speck, A. K., Onaka, T., 2001, ApJ, 733, 93.

Guha Niyogi, Suklima; Speck, Angela K.; Volk, Kevin, 2011, Astronomical Review, 6, 27.

1975 Opt. Soc. Am. 65, 742.

Henning, T. Il'In, V. B., Krivova, N. A., Michel, B., Voshchinnikov, N. V., 1999, A&A, 136, 405.

Henning, Th. K., ed. 2003, Astromineralogy, Lecture Notes in Physics 609, Springer, Heidelberg.

Henning, Th. K., 2010, ARA&A, .48, 21.

Henning, Th., Mutschke, H. 1997, A&A, 327, 743.

Henning, Th., Stognienko, R. 1993 A&A, 280, 609.

Hofmeister, A. M.; Pitman, K. M.; Goncharov, A. F.; Speck, A. K. 2009, ApJ, 696, 1502.

Hofmeister A.M., Keppel E., Speck A.K. 2003, MNRAS, 345, 16.

Hoozgaad, S.N., Molster, F.J., Dominik, C., Waters, L.B.F.M., Barlow, M.J., de Koter, A. 2002, A&A, 389, 547.

Hrivnak, Bruce J.; Kwok, Sun; Volk, Kevin M. 1989, ApJ, 346, 265,

Huffman, D. R., 1975, Ap&SS, 34, 175.

Huffman, D. R., Stapp, J. L. 1973, in Interstellar Dust and Related Topics. IAU Symp. 52, (Eds) J. Mayo Greenberg and H. C. van de Hulst. Dordrecht, Boston, Reidel, p.297

Ivezic, Z. & Elitzur, M. 1995, ApJ, 445, 415.

Iwamoto, Koichi; Brachwitz, Franziska; Nomoto, Ken'ICHI; et al. 1999, ApJS, 125, 439.

Jäger, C., Mutschke, H., Begemann, B., Dorschner, J., Henning, Th. 1994, A&A, 292, 641.

Jones, A. P.; Nuth, J. A. 2011, A&A, 530, 44.

Justtanont, K.; Barlow, M. J.; Skinner, C. J.; Tielens, A. G. G. M. 1992, ApJ, 392, L75.

Kim, Sang-Hee; Martin, P. G. 1995, ApJ, 442, 172.

Kim, Sang-Hee; Martin, P. G., Hendry, Paul D. 1994, ApJ, 422, 164.

Kyotyukh, V.V., 2007, MNRAS, 378, 617.

Krätschmer, W., Huffman, D. R. 1979, Ap&SS, 61, 195.

Kwok, S. 2004, Nature, 430, 985.

Lang, K.R., 1992, Astrophysical Data I: Planets and Stars, X, 937 pp, Springer-Verlag Berlin.

Laor, A. Draine, B.T., 1993, ApJ, 402, 441.

Li, Aigen; Draine, B. T. 2001, ApJ, 554, 778.

Lodders, K., Fegley, B., Jr. 1999, in IAU Symp. 191, Asymptotic Giant Branch Stars, ed. T. Le Bertre, A. Lebre, C. Waelkens (New York: Springer), 279

Lynch, D.W. and Hunter, W. R., 1991, In: Handbook of Optical Constants of Solids II, edited by E. D. Palik (Orlando: Academic Press), pp. 341-377;

Lyubimkov, L.S., Lambert, D.L., Rostopchin, S.I., Rachkovskaya, T.M., Poklad, D.B., 2010, MNRAS, 402, 1369.

Mathis, J. S., Rumpl, W., & Nordsieck, K. H. 1977, ApJ217, 425.

Mathis, J.S., Mezger, P. G., Panagia, N., 1983, A&A, 128, 212

Meixner, M., Ueta, T., Bobrowsky, M., & Speck, A. 2002, ApJ, 571, 936.

Men'shchikov, A. B.; Schertl, D.; Tuthill, P. G.; Weigelt, G.; Yungelson, L. R. 2002, A&A, 393, 867.

Merrill K.M., Stein W.A. 1976, PASP, 88, 285.

Merzbacher C.I., White W.B. 1988, American Mineralogist, 73, 1089.

Min, M., Waters, L. B. F. M., de Koter, A., et al. 2007, A&A, 462, 667

Min, M., Hovenier, J. W., de Koter, A, 2003, A&A, 404, 35.

Molster, F. J. 2000, "Crystalline Silicates in Circumstellar Shells" Ph.D. thesis. see: http://dare.uva.nl/en/record/88466

Monnier, J. D., Geballe, T. R., Danchi, W. C. 1998, ApJ, 502, 833.

Nenkova, M., Ivezic, Z., & Elitzur, M. 2000 in ASP Conf. Ser. 196, Thermal Emission Spectroscopy and Analysis of Dust, Disks, and Regoliths, ed. M. L. Sitko, A.L. Sprague & D. K. Lynch (San Fransicso: ASP), 77.

Nomoto, Ken'ichi; Tominaga, Nozomu; Umeda, Hideyuki; Kobayashi, Chiaki; Maeda, Keiichi 2006, Nuclear Physics A, 777, 424.

Ordal et al., 1988, Appl.Opt. 27, 1203.

Ossenkopf, V., Henning, Th., & Mathis, J. S. 1992, A&A, 261, 567.

Palik, Edward D., 1985 Handbook of Optical Constants of Solids, Academic Press, Jun 17, 1985, 804 pages

Palik, Edward D., 1991 Handbook of Optical Constants of Solids, II, Academic Press, April 4, 1991, 1096 pages

Papoular, R., Pégourié, B. 1983, A&A, 128, 335.

Pégourié, B. 1988, A&A, 194, 335.

Pinte, C., Padgett, D. L., Mnard, F., et al. 2008, A&A, 489, 633.

Pitman, K. M., Speck, A. K., Hofmeister, A. M., Buffard, A. S., Whittington, A. G., 2013, American Astronomical Society, AAS Meeting #221, #223.04

Pitman, K. M., Hofmeister, A. M., and Speck, A. K. 2013, Earth, Planets and Space, 65, 129.

Pitman, K. M., Dijkstra, C., Hofmeister, A. M., and Speck, A. K. 2010, MNRAS., 406, 460.

Pitman, K. M., Hofmeister, A. M., Corman, A.B., Speck, A. K., 2008, A&A, 483, 661.

Pollack, James B.; Hollenbach, David; Beckwith, Steven; et al. 1994, ApJ, 421, 615.

Rogers C., Martin P.G., Crabtree D.R. 1983, ApJ, 272, 175.

1991, "Glass: Nature, Structure, and Properties" New York : Springer-Verlag, 454 pages

Scott, A., Duley, W. W. 1996, ApJS, 105, 401.

Skinner, C.J., Meixner, M.M., Hawkins, G.W., Keto, E., Jernigan, J.G., Arens, J.F., 1994, ApJ, 423, L135.

Sorrell, Wilfred H. 1990, ApJ, 361, 150.

Speck, A. K., 2014, "Modeling Cosmic Dust: How to Use Optical 'Constants' " in Proceedings of Science Vol ## - Proceeding of Lifecycle of Dust in the Universe.

Speck, A. K., 2012, JAVSO, 40, 244.

Speck, Angela K.; Whittington, Alan G.; Hofmeister, Anne M. 2011,ApJ, 740, article id. 93, 17 pp.

Speck, Angela K., Corman, Adrian B., Wakeman, Kristina, Wheeler, Caleb H., Thompson, Grant 2009, ApJ, 691, 1202.

Speck, A. K., Barlow, M. J., Sylvester, R. J., Hofmeister, A. M. 2000, A&AS, 146, 437.

Speck, A. K., Hofmeister, A. M., Barlow, M. J. 1999, ApJ, 513, L87.

Speck, A. K. 1998, PhD Thesis. University College London,

Speck, A. K., Barlow, M. J., Skinner, C. J. 1997, MNRAS288, 431.

Spitzer, W. G.; Miller, Robert C.; Kleinman, D. A.; Howarth, L. E. 1962, Phys. Rev., 126, 1710.

Suh, K.-W. 1991, Ap&SS, 181, 237.

Sylvester, R. J., Kemper, F., Barlow, M. J., et al. 1999, A&A, 352, 587.

Ueta, T., Meixner, M., Dayal, A., et al. 1999, ApJS, 122, 221.

Volk, K., Kwok, S., 1988, ApJ, 331, 435.

Voors, R. H. M.; Waters, L. B. F. M.; de Koter, A., et al. 2000, A&A, 356, 501.

Voshchinnikov, N. V., Henning, T. 2008, A&A, 483, L9.

Waters, L. B. F. M., and Molster, F. J. 1999, in Asymptotic Giant Branch Stars, eds. T. Le Bertre, A. Lbre, and C. Waelkens, IAU Symp. 191, Astron. Soc. Pacific, San Francisco, 209.

Wooten, F. 1972, Optical Properties of Solids (New York: Academic Press).

Young, K., Phillips, T.G., Knapp, G.R. (YPK) 1993, ApJ, 409, 725.

Zhukovska, Svitlana "Dust formation by stars and evolution in the interstellar medium"

2008, PhD Thesis. Ruprecht-Karls-Universitt Heidelberg, pp169.

This 2-column preprint was prepared with the AAS LaTeX macros v5.2.

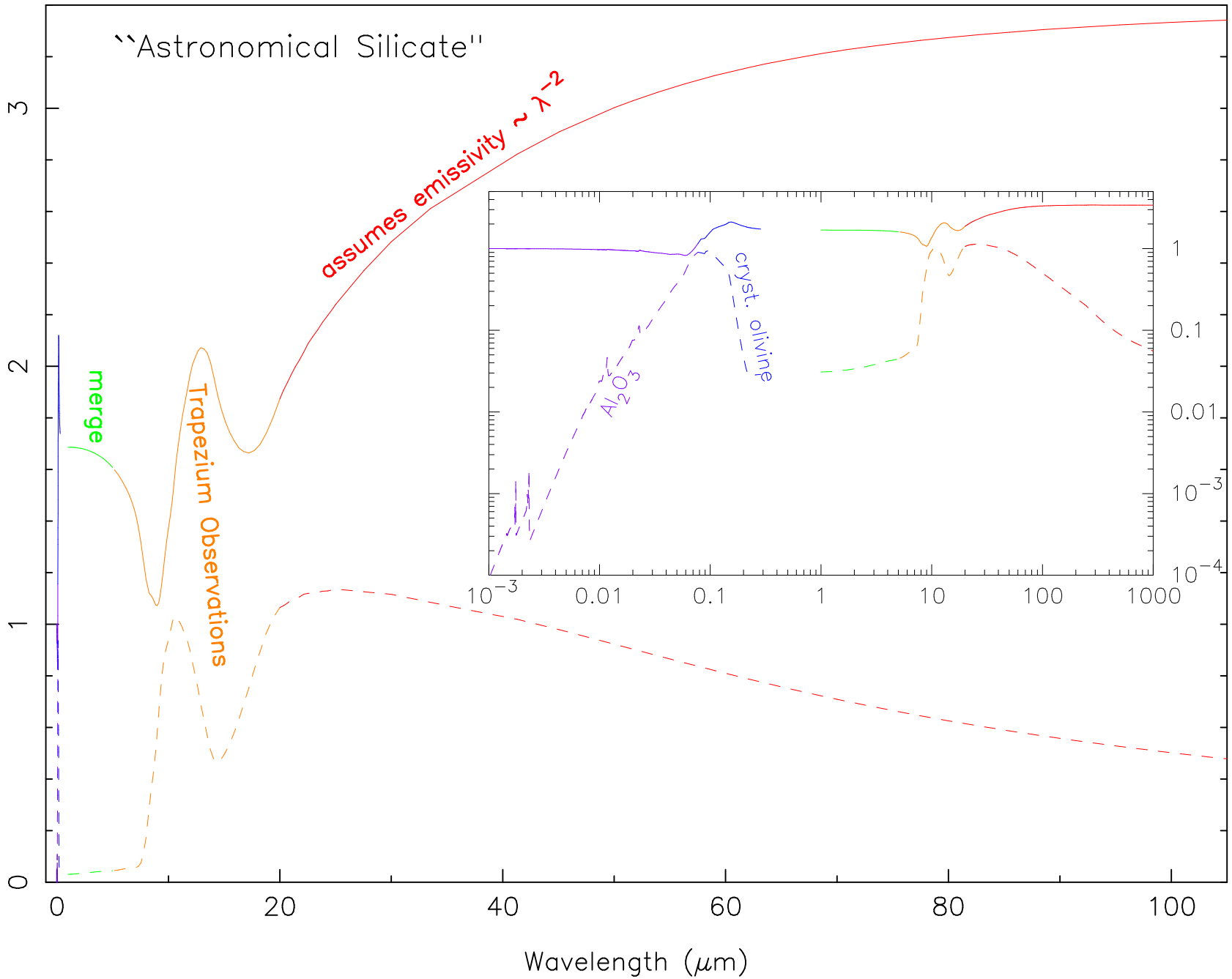
``Astronomical Silicate''
assumes emissivity ~ λ^-2
merge
Trapezium Observations
cryst. olivine
Al2O3
0
1
2
3
0
20
40
60
80
100
Wavelength (μm)
10^-3
0.01
0.1
1
10
100
1000
1
0.1
0.01
10^-3
10^-4